OFFICE OF NAVAL RESEARCH

TECHNICAL REPORT

ADVANCED TECHNOLOGY FOR IMPROVED QUANTUM DEVICE PROPERTIES USING HIGHLY STRAINED MATERIALS

GRANT NUMBER:

N00014-89-J-1386

FOR THE PERIOD

DECEMBER 15, 1988 TO JUNE 15, 1989

CORNELL UNIVERSITY

ITHACA, NY 14853-5401

PREPARED BY:

W.J. Schaff

S.D. Offsey

H. Park

L.F. Eastman

Table of Contents

ADVANCED TECHNOLOGY FOR IMPROVED QUANTUM DEVICE PROPERTIES USING HIGHLY STRAINED MATERIALS

Strained layer GaInAs/GaAs heterostructures for improved high frequency high performance as a result of strained modified valence band structure have been investigated. A new laser structure has been successfully developed which permits direct high frequency modulation of non wire-bonded lasers. The first demonstration of improved microwave frequency bandwidths for lasers has been achieved. Substantial improvement in bandwidth for strained GaInAs quantum well graded index separate confinement heterostructure lasers over unstrained GaAs quantum well lasers has been measured, accompanied by a reduction in threshold current densities for lasing. Strained P-channel MODFETs have been fabricated, but show no significant improvement in high frequency performance. Fundamental materials properties of strained layer GaInAs quantum wells are being investigated and theoretical examination of the properties of strained layer quantum wells are being conducted.

Strained layer GaInAs single quantum well graded index separate confinement heterostructure (GRINSCH) lasers

Lattice mismatched heteroepitaxy is of great interest since it provides increased flexibility for band gap engineering. Strained-layer quantum wells have been used to control the band gap of the active region ot semiconductor lasers,[1,2,3,4] thereby permitting lasing at previously unattainable wavelengths and allowing optical pumping of solid state glass lasers, for example. Moreover, recent studies have confirmed a splitting of the valence bands leading to a reduction in the hole mass parallel to the junction in the strained GaAs-$Ga_xIn_{1-x}As$-GaAs quantum well.[5,6] Theoretical studies predict that the lower

density of states in the light hole band would allow the population inversion needed for lasing to occur at lower threshold currents for strained-layer lasers.[7,8,9] These lower threshold currents would lead to an increase in high speed performance over lasers made from unstrained material.[9] In this first series of design, growth, fabrication and measurement of strained-layer graded-index separate-confinement heterostructure (GRINSCH) single quantum well (SQW) lasers improvement over unstrained structures is clearly demonstrated.

Direct modulation of semiconductor lasers for transmitting microwave, and eventually millimeter wave frequency modulation, will require low threshold current operation to permit maximum optical output power with minimum power dissipation. The highest frequency performance will be obtained with structures which use the smallest dimensions of cavity length and width. Lowest threshold current densities at shorter cavity lengths (<500μm) are obtained in graded index separate confinement heterostructure (GRINSCH) lasers compared to double heterostructure (DH) laser designs. Since the eventual goal of this 3 year grant is to obtain near 60 GHz modulation, short cavity lengths (<200μm) will be utilized, thus GRINSCH structures are employed.

The first strained quantum well GRINSCH laser structures to be studied, shown in figure 1, were grown on an n^+ substrate by molecular beam epitaxy (MBE): (1) a 1500 Å Si doped GaAs buffer ($n = 4 \times 10^{18}$ cm^{-3}) grown at 580 °C, a 1500 Å Si doped region ($n = 2 \times 10^{18}$ cm^{-3}) grown at 710 °C graded to $Al_{0.7}Ga_{0.3}As$, and a 1.2 μm Si doped $Al_{0.7}Ga_{0.3}As$ lower cladding region ($n = 2 \times 10^{18}$ cm^{-3}) grown at 710 °C, (2) a GRINSCH active region consisting of a 4000 Å $Al_xGa_{1-x}As$ layer graded from x = 0.7 to x = 0.3 grown at 710 °C, a growth interruption for 2 minutes, an undoped 10 Å GaAs layer grown at 500 °C, an undoped 50Å $Ga_{0.7}In_{0.3}As$ quantum well grown at 500 °C, another undoped 10 Å GaAs layer grown at 500 °C, a 2 minute growth interruption while the substrate temperature was ramped up to 710 °C, and a 4000 Å $Al_xGa_{1-x}As$ layer graded from x = 0.3 to x = 0.7 grown at 710 °C, (3) a 1.2 μm Be doped $Al_{0.7}Ga_{0.3}As$ upper

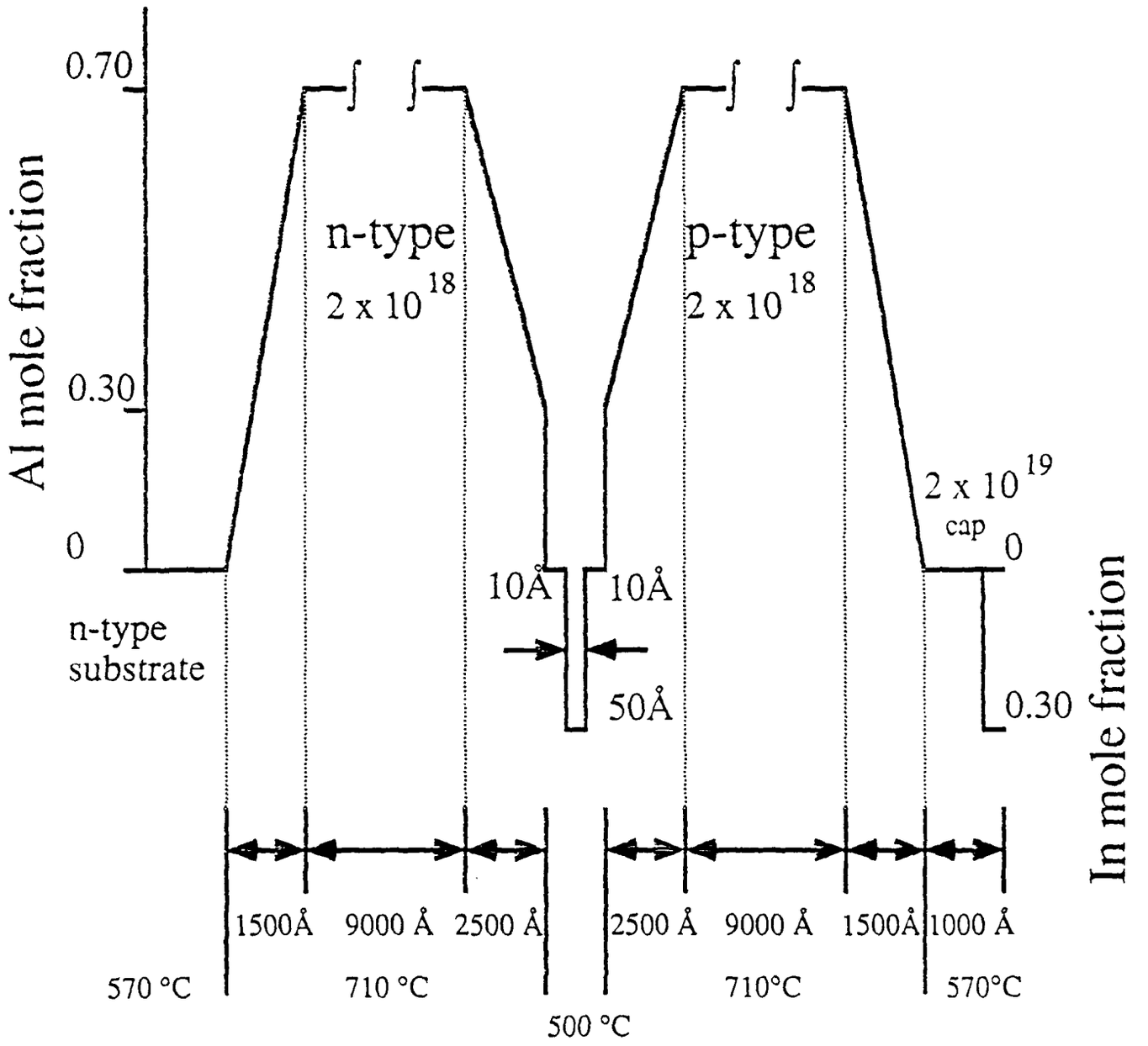

Figure 1. Composition profile fo the strained-layer $Ga_{0.7}In_{0.3}As$ graded-index separate-confinement heterostructure single quantum well laser.

[illegible] region ($p = 2 \times 10^{18}$ cm^{-3}) grown at 710 °C, a 1500 Å Be doped layer graded to [illegible] ($p = 2 \times 10^{18}$ cm^{-3}) grown at 710 °C, and a 5000 Å Be doped GaAs cap ($p = 2 \times 10^{19}$ cm^{-3}) grown at 570 °C. Throughout the entire structure the $Al_xGa_{1-x}As$ regions were interrupted by thin GaAs layers (290 Å $Al_xGa_{1-x}As$, 10 Å GaAs). The growth rate for GaAs was 0.5 μm per hour throughout.

The first processing step in the fabrication of the lasers was a mesa isolation by chemically etching down to the n^+ GaAs region. Cavity widths were produced ranging from 3 to 40 μm. MnZnAu p-type metallization and AuGeNi n-type metallization were each defined by lift-off and then alloyed. After the wafers were thinned they were cleaved into bars ranging from 200 - 1200 μm long.

A 300 K spectrum for a 40 μm x 800 μm laser is shown in figure 2. This laser was driven at twice its threshold current under pulsed conditions with a 10% duty cycle and shows a multi-mode emission centered at a wavelength of 1.026 μm. This wavelength corresponds to a transition energy of 1.21 eV which is the photon emission energy calculated by Kolbas, *et. al.* [4] for a 50 Å $Ga_{0.7}In_{0.3}As$ quantum well grown on GaAs. This agreement confirms that all the indium incident on the substrate during GaInAs growth was incorporated into the quantum well. Figure 3 contains a continuous wave (cw) spectrum for a 40 μm x 800 μm device which demonstrates single mode emission. The cw spectrum exhibits a wavelength shift of 21 nm from the pulsed spectrum, indicating significant heating of these non thermally bonded devices.

Figure 2 also contains the data from a typical optical power versus current measurement for a 3 μm x 400 μm laser. For the measurements of optical power versus current the lasers were driven by 3 μsec wide pulses at 1 kHz in order to avoid the deleterious effects of heating caused by cw operation. The lasers have typical threshold currents of 12 mA for 3 μm x 300 μm wide devices while the average threshold current density of 40 μm x 800 μm devices is 174 A/cm^2. The results of a study of threshold current versus cavity length are shown in figure 4. The theoretical curves are obtained

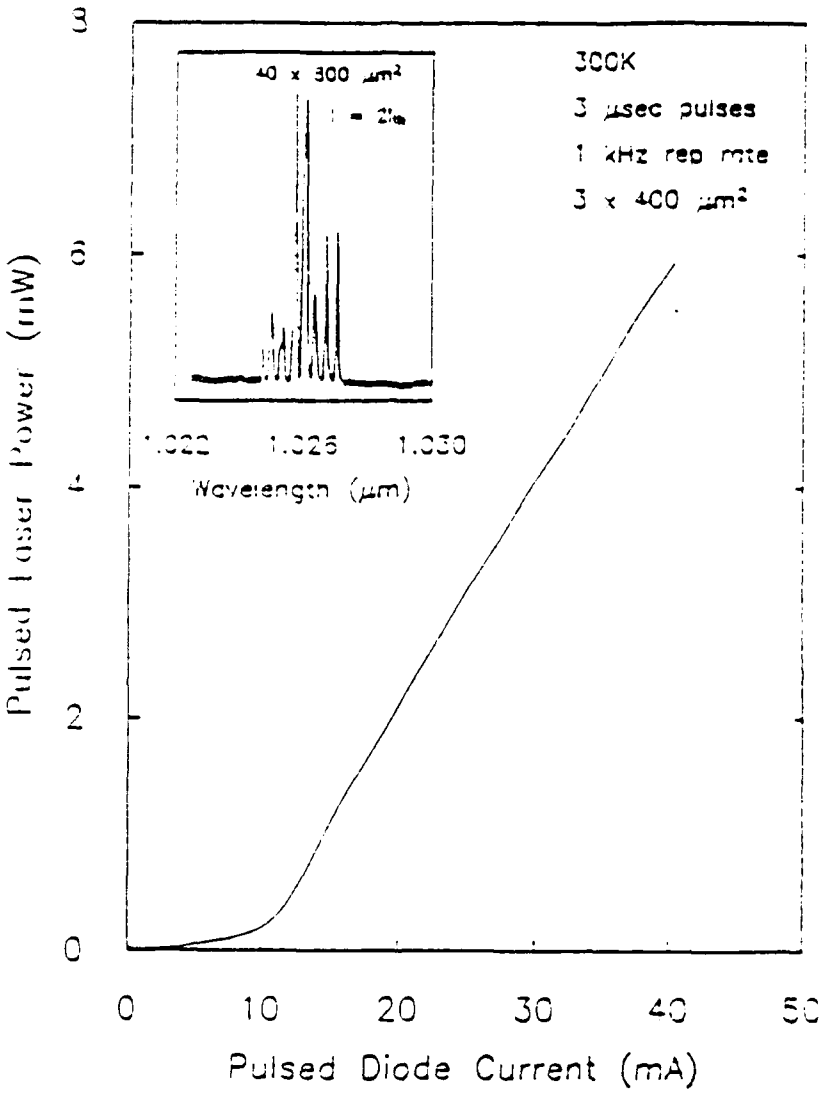

Figure 2. Pulsed power verses current (3 usec pulses at 1 kHz) for a 3 um x 400 um device at 300K. Included is a 300 K pulses spectrum for a 40 um x 800 um device.

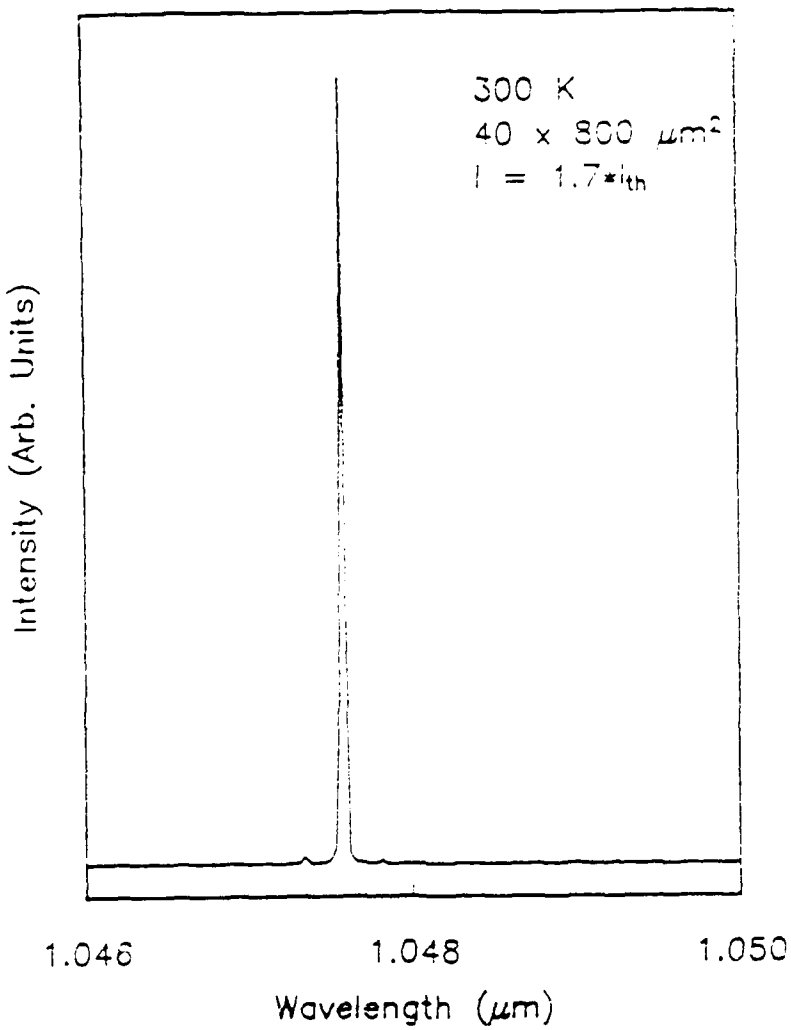

Figure 3. A room temperature CW spectrum for a 40 um x 80 um device operating at 100mA.

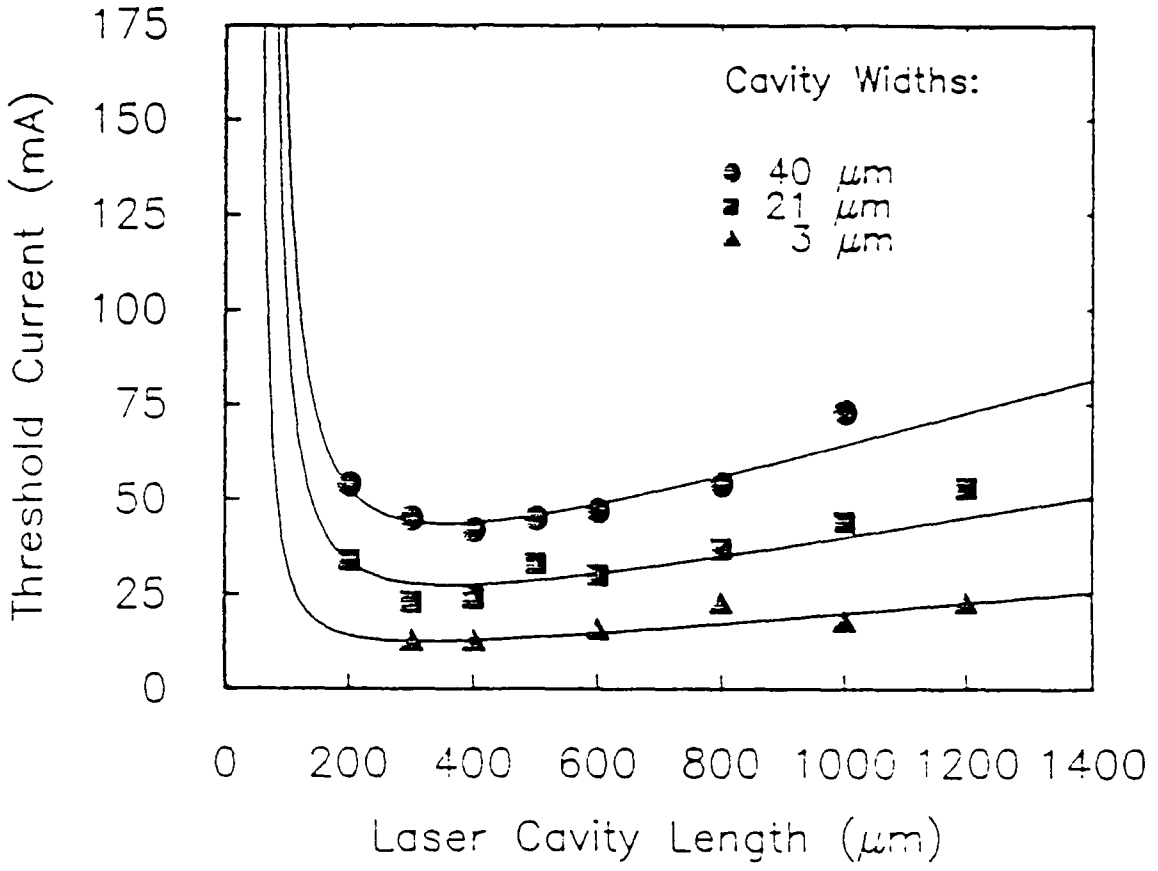

Figure 4. Threshold current verses cavity length. The solid curves are derived using equations 1, 2, and 3.

using the following equations which are derived in references [10] and [11]. A linear fit can be obtained when the natural log of the current density is plotted verses cavity length as shown in equation 1.

$$\ln J_{th} = \frac{L_{opt}}{L} + \left\{ \frac{\alpha}{\Gamma G_o} + \ln\left(\frac{J_o}{\eta_i}\right) - 1 \right\} \tag{1}$$

$$L_{opt} = \frac{\ln R^{-1}}{\Gamma G_o} \tag{2}$$

where J_{th} is the current density (A/cm^2), L_{opt} is the cavity length resulting in the lowest threshold current, L is the cavity length, α is the intrinsic optical loss, Γ is the modal confinement factor, J_o and G_o are the saturation current and saturation gain as defined in reference [10], η_i is the intrinsic quantum efficiency, and R is the mirror reflectivity (R = 0.3 for uncoated facets). The slope of the plot of J_{th} verses L gives the value of $(\Gamma G_o)^{-1}$ and the intercept gives the value of the bracketed portion of equation 1. The theoretical curves for the threshold current used in figure 4 are determined by using equations 1 and 2, the relation

$$I_{th} = WLJ_{th} \tag{3}$$

where W is the cavity width, and the constants determined as described above. It can be seen from figure 4 that this theory applies to strained-layer quantum well lasers equally as well as to the unstrained quantum well lasers in reference [11]. The optimal cavity lengths, L_{opt}, for the 3 μm, 21.5 μm and 40 μm wide lasers were determined from equation 2 to be 314 μm, 354 μm and 358 μm, respectively.

Equation 3 and other theoretical studies[12] predict that threshold current is proportional to cavity width. This relationship was confirmed for each of the cavity lengths used in this

study and data for 300, 400 and 600 μm long cavities are shown in figure 5. It can be seen from figures 4 and 5 that threshold currents show much more variation with cavity width than with cavity length for typical cavity lengths between 200 and 800 μm. Therefore the most appropriate way to compare lasers from different studies is to show them on a plot of threshold current verses cavity width. Figure 5 shows that the lasers in this study have lower threshold currents than previously published strained-layer lasers grown by MBE.[13] These lasers also have threshold currents below strained-layer lasers grown by OMVPE.[3,14]

Improvement in threshold density for strained QW lasers compared to GaAs QW lasers is seen in figure 6. This improvement in threshold is seen for all strained QW lasers fabricated during this study to date for In mole fractions greater than 25%. In our lab, we have had no success fabricating lasers from quantum wells with compositions greater than 0% and less than 20%. Two growths at 20% and one at 10% produced either very high thresholds, or no lasing action. The reason for this poor performance of low In mole fraction devices is not clear. These may be simple statistical failures due to the very small number of attempts at these compositions (although wafer to wafer yields are 100% for In compositions of 25% and 35%). Because improvements due to strain are maximized at high In mole fractions, no significant effort will be expended in the future to explain this phenomena - especially since informal discussions with others in the field lead us to believe that this behavior is peculiar to our lab. Fundamental materials studies in progress which cover low In mole fractions in addition to high mole fractions show no unusual characteristics to explain composition dependant growth problems. These studies will be completed and reported during 1990.

These low threshold currents are believed to be due to a separate optimization of the growth conditions for the $Al_xGa_{1-x}As$, GaInAs and the interface between them. The growth conditions for the quantum well were selected as a result of previous studies that evaluated the growth conditions for strained-layer GaInAs on GaAs.[15,16] Growth was

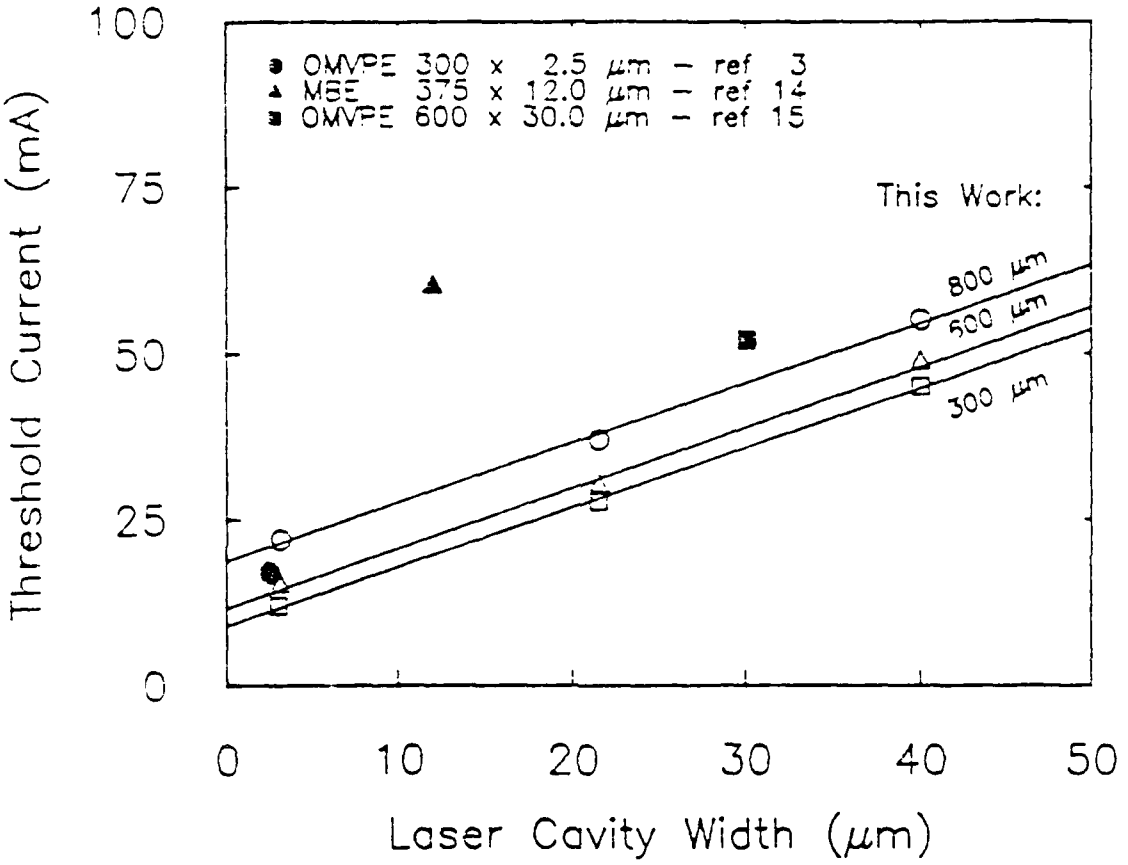

Figure 5. Threshold current verses cavity width. The solid lines are least squares fits to the data from this study. The cavity lengths that are shown most closely correspond to those of the lasers from references 3, 13, and 14.

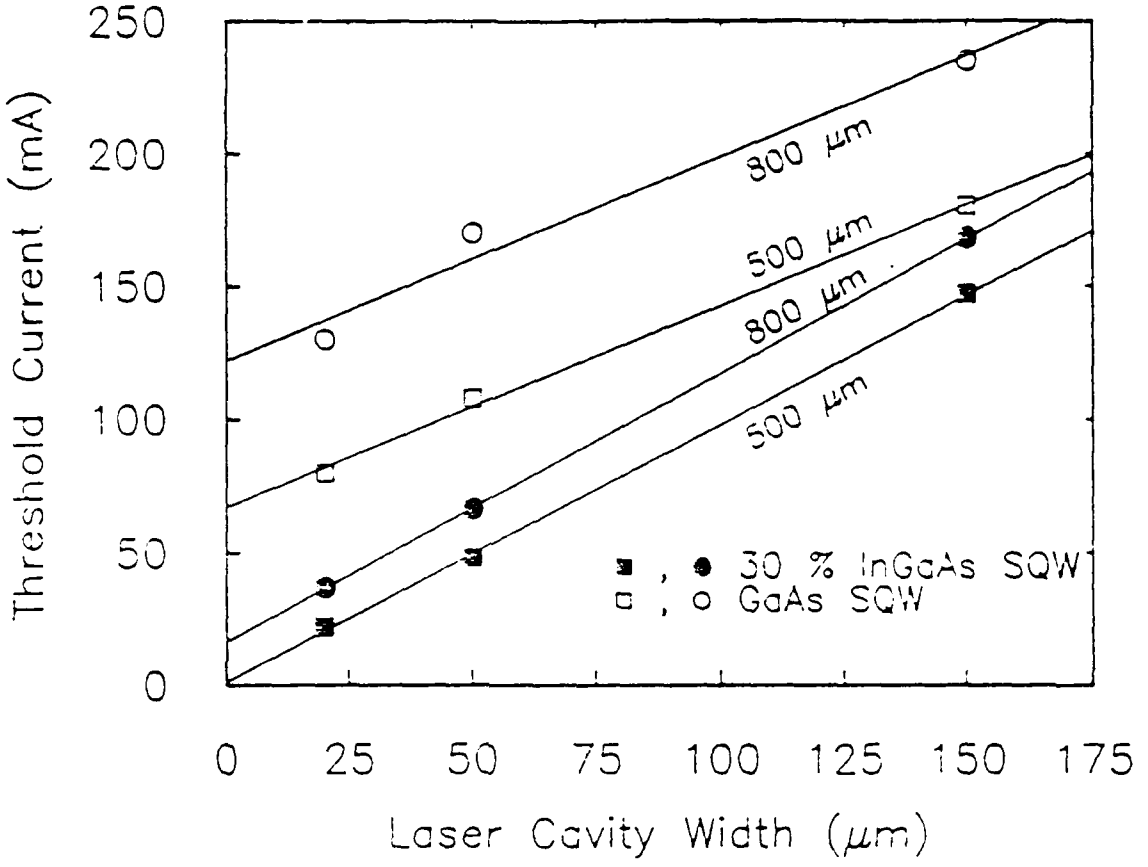

Figure 6. Threshold current verses cavity width for 20 um wide unstrained GaAs and strained layer $In_{0.30}Ga_{0.70}As$ lasers.

stopped for 2 minutes before the 10 Å GaAs layer in order to obtain a smooth interface and allow for the substrate temperature to stabilize. The GaInAs quantum well was grown at the relatively low temperature of 500 °C to prevent the indium from either segregating or 'riding' the growing interface. After the upper 10 Å GaAs layer was grown, another 2 minute growth interruption was performed while the substrate temperature was increased. Previous growth studies showed degraded mobilities in quantum well MODFETs grown on thick AlGaAs buffers due to impurities and defects.[17] Therefore the $Al_xGa_{1-x}As$ regions were grown with frequent thin GaAs regions throughout in order to smooth the growing surface and getter electronically active impurities and defects[18] which could raise the threshold currents of the lasers.

Laser Microwave Performance

The continuous wave (cw) microwave modulation response of the strained and unstrained devices was measured by non-bonded direct probing using a Cascade Microtech microwave probe. The laser structure developed during this study to permit the first non-bonded microwave laser measurements is shown in figure 7. Direct probing of the devices permits the dc and microwave characteristics of large numbers of devices to be measured without the large parasitic capacitances and inductances associated with wire bonding. Figure 8 shows the microwave modulation response of a 10 μm x 500 μm InGaAs strained layer laser at multiple current levels. The characteristic increase and broadening of the relaxation modulation frequency with increasing current is observed with a maximum -3 dB cutoff point of almost 6 GHz.

The -3 dB cutoff frequency is plotted versus the square root of the single facet optical power for 20 μm x 800 μm InGaAs strained layer and GaAs unstrained lasers in figure 9. The characteristic linear relationship between bandwidth and the square root of photon density or optical power is observed for each device. The strained layer device in figure 9 shows a bandwidth greater than that of the GaAs unstrained laser at each corresponding

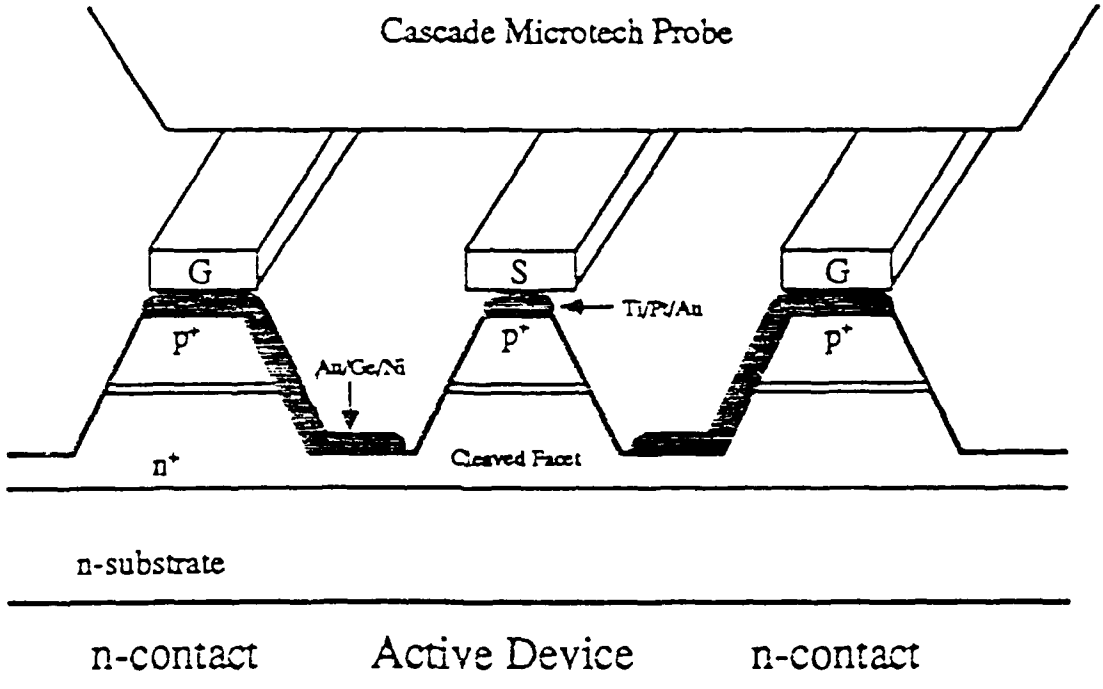

Figue 7. An edge on schematic of the laser structure showing the three mesa ground-signal-ground configuration and the Cascade Microtech probe.

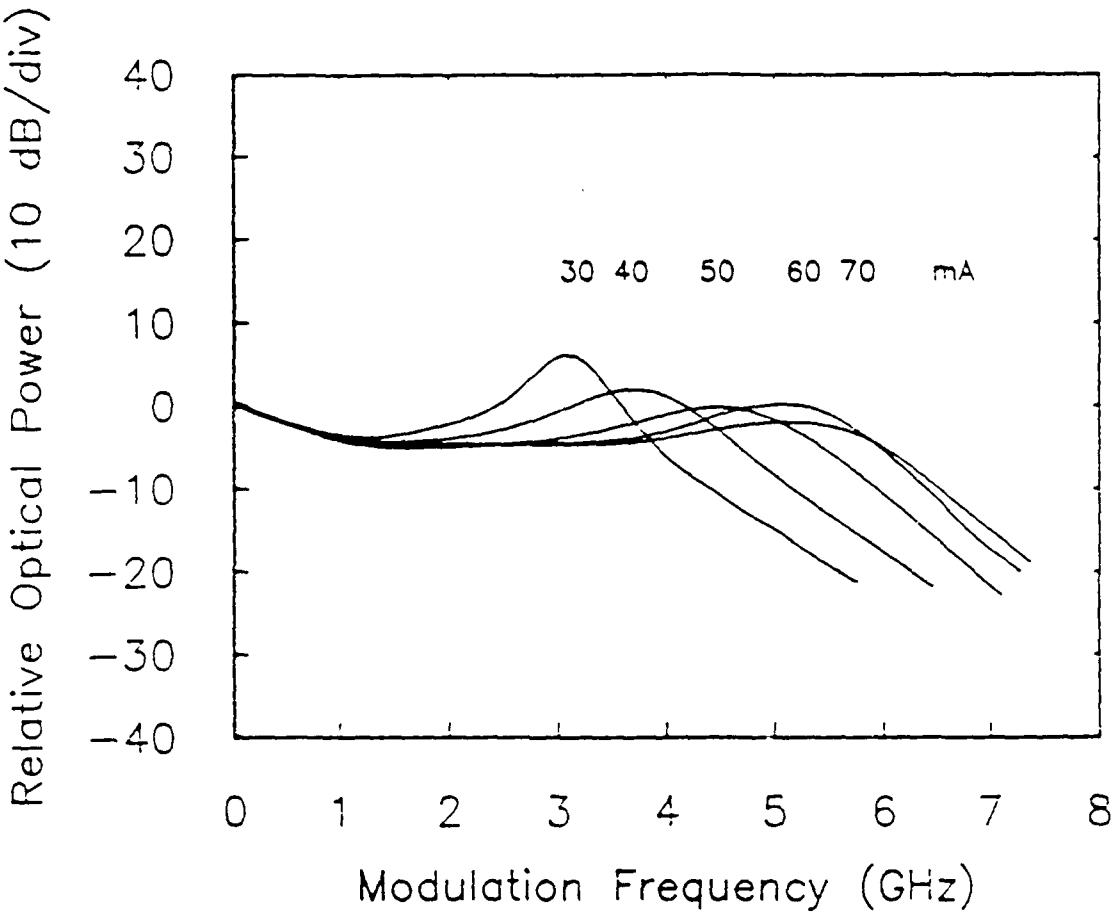

Figure 8. Microwave modulation response for a 10 um x 500 um strained layer $In_{0.30}Ga_{0.70}As$ laser at 30, 40, 50, 60 and 70 mA.

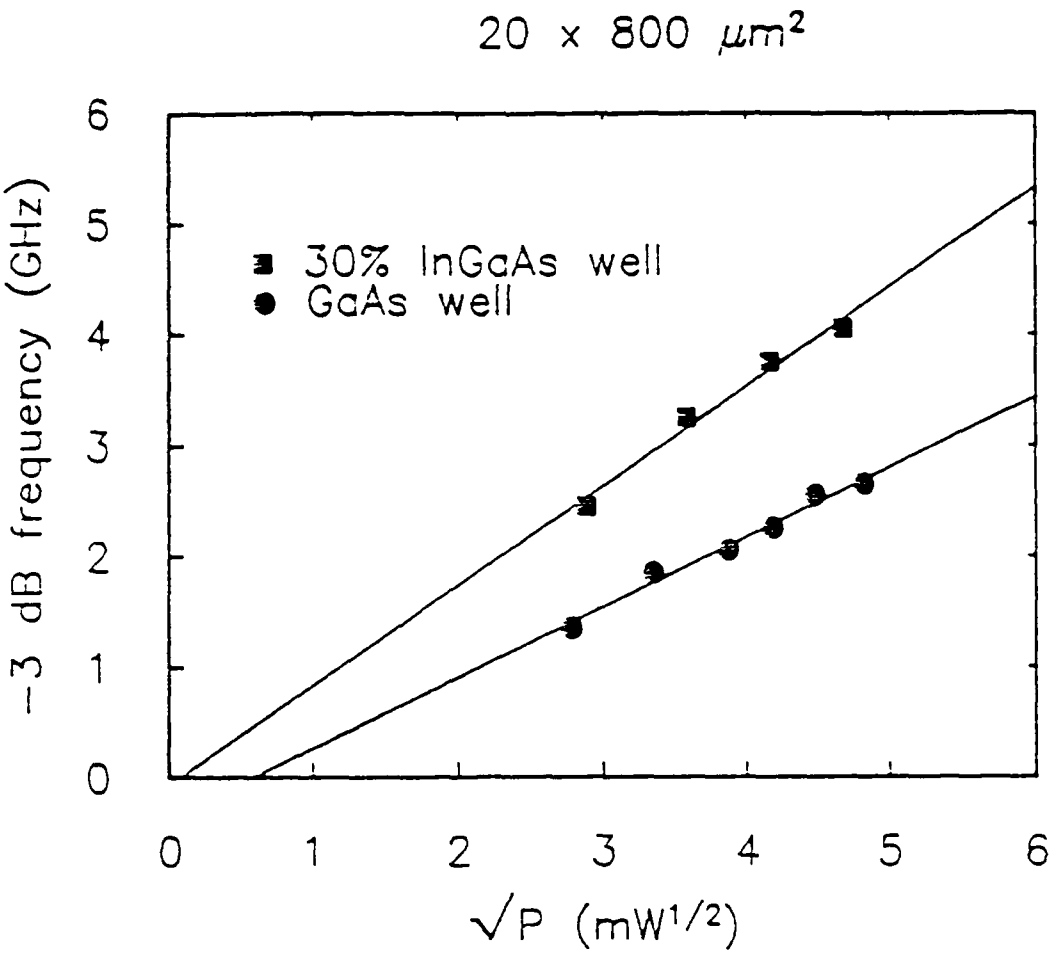

Figure 9. Comparison of -3 dB bandwidth versus the square root of single facet optical power for unstrained GaAs and stained layer $In_{0.30}Ga_{0.70}As$ 20 um x 800 um lasers.

optical power level. Figure 10 contains the same plot of bandwidth versus the square root of single facet optical power for two 20 μm x 500 μm lasers. For these lasers, as well as for all the devices measured, the bandwidth of the InGaAs strained layer laser was higher than the bandwidth of the GaAs unstrained laser. These results confirm the theoretical prediction made in reference 9 that the reduction in the hole mass due to biaxially compressive strain will result in higher modulation bandwidths for strained layer lasers.

Strained P-Channel MODFETs

Modulation doped field effect transistors (MODFET)s using strained GaInAs p-channels have been studied. Two improvements over GaAs channel MODFETs were sought. First, the reduced hole mass as a result of strain was desired to improve channel conductivity. Second, the improved valence discontinuity between the AlGaAs hole supply layer and GaInAs channel would be expected to improve hole confinement to the channel. Devices using strained p-channel MODFETs will be fabricated on layers grown during this period. Results will be included in the next report.

Theoretical description of strained quantum wells

The light mass of holes in the region of about .050 eV depth into the valence band of strained In,GaAs quantum wells grown on GaAs is of great interest. Professor Brian K. Ridley will be in residence at Cornell for three months in early 1990 initiating the theory of such structures. He will return for two months for each of the next three years. In the future, the results of this theory will be the key to the theoretical development on this program.

Materials properties of strained GaInAs

The growth of strained GaInAs on GaAs will be studied by low temperature photoluminescence (PL). Substrate temperatures will be varied from 300C to 500C. Post

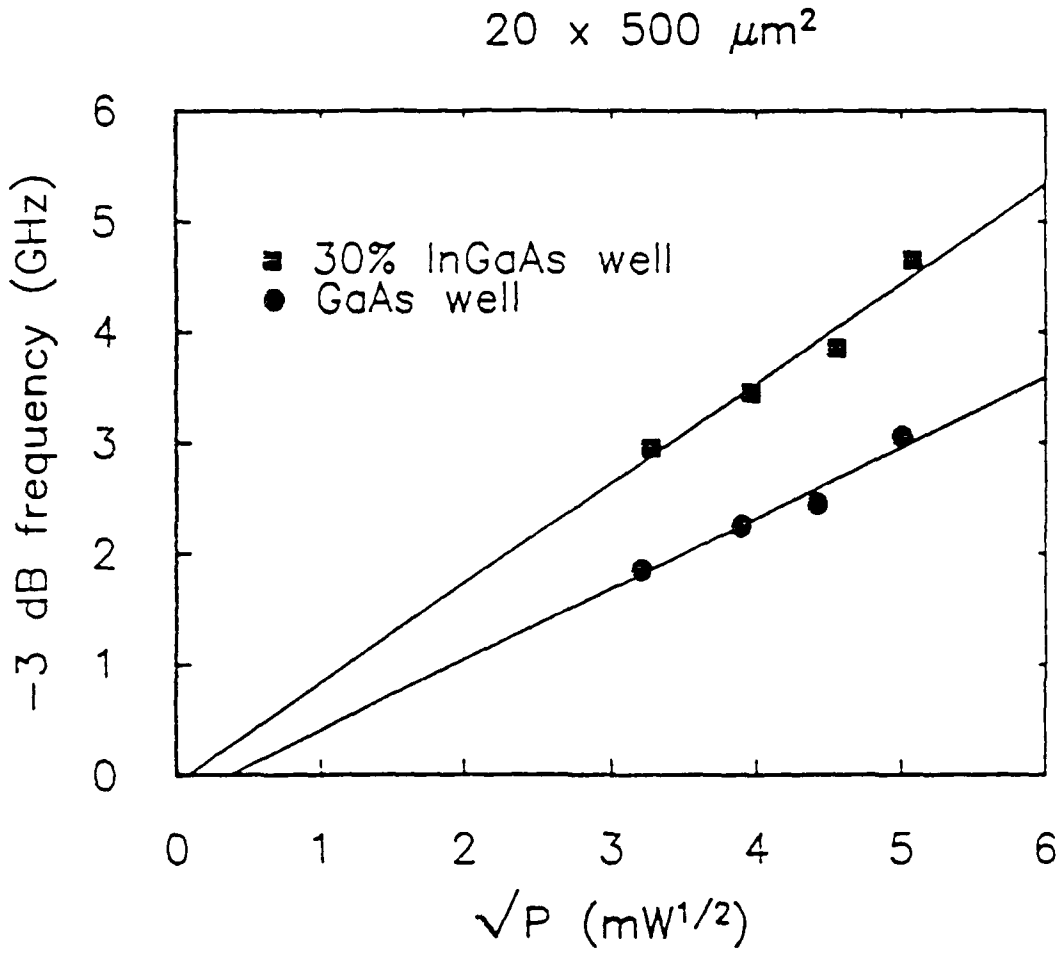

Figure 10. Comparison of -3 dB bandwidth versus the square root of single facet optical power for unstrained GaAs and strained layer $In_{0.30}Ga_{0.70}As$ 20 um x 500 um lasers.

growth annealing will be performed. Strained GaInAs quantum wells with AlInAs and AlGaInAs barriers will be grown on InP to study their properties for application to lasers. Theoretical predictions are for further improvement in threshold current densities and modulation bandwidths for these materials. They will be evaluated by low temperature PL and TEM. Critical thicknesses will be studied for this material system.

Ongoing research, near future plans

Completion of the study of growth conditions of strained GaInAs/GaAs quantum wells will occur in 1990. Research into strained layer AlInAs/GaInAs/InP quantum wells will continue. Lasers will be fabricated in this material system. The goal of these devices is to further improve laser performance due to valence band modification of strained layer GaInAs on InP which will offer valence band structure with better properties than strained GaInAs on GaAs. The lasing wavelengths will also be more valuable for 1.55μm fiber applications.

Multiple QW GaInAs/GaAs lasers will be explored to determine their suitability to short cavity length devices. Superior high frequency performance is the goal of this effort. Portions of laser materials fabricated under this grant will be supplied to an ongoing program by GE at Cornell in 1990 to fabricate dry etched laser mirrors for short cavity length applications.

Papers and presentations supported by this grant

1. "Strained-Layer InGaAs-GaAs-AlGaAs Graded-Index Separate-Confinement Heterostructure Single Quantum Well Lasers Grown by Molecular Beam Epitaxy", S.D. Offsey, W.J. Schaff, P.J. Tasker, H. Ennen and L.F. Eastman, *Appl. Phys. Lett.* **54**, (25) 2527-2529 (June 1989).

2. "Strained-Layer InGaAs-GaAs-AlGaAs Graded-Index Separate-Confinement Single Confinement Single Quantum Well Lasers Grown by Molecular Beam Epitaxy", S.D. Offsey, W.J. Schaff, P.J. Tasker and L.F. Eastman, *Device Research Conference*, MIT, Cambridge, MA (June 19-21, 1989).

REFERENCES

1. W. D. Laidig, Y. F. Lin, P. J. Caldwell, J. Appl. Phys. **57**, 33 (1985).
2. D. Feketa, K. T. Chan, J. M. Ballantyne, and L. F. Eastman, Appl. Phys. Lett. **49,** 1659 (1986)
3. S. E. Fischer, D. Fekete, G. B. Feak, and J. M. Ballantyne. Appl. Phys. Lett. **50,** 714, (1987)
4. R. M. Kolbas, N. G. Anderson, W. D. Laidig, Y. Sin, Y. C. Lo, K. Y. Hsieh, and Y. J. Yang. IEEE J. Quantum Electron. **QE-24**, 1605 (1988)
5. J. Hwang, C. K. Shih, P. Pianetta, G. D. Kubiak, R. H. Stulen, L. R. Dawson, Y. C. Pao, and J. S. Harris. Appl. Phys. Lett. **52**, 308 (1988)
6. E. D. Jones, S. K. Lyo, J. F. Klem, J. E. Schirber, C. P. Tigges. Proc. Inst. Phys. Conf. Ser. vol. **96** (1989)
7. A. R. Adams. Electron. Lett. **22** , 250 (1986)
8. E. Yablonovitch, E. O. Kane. J. of Lightwave Tech. **LT-4**, 504 (1986), see also correction J. of Lightwave Tech. **LT-4**, 961 (1986)
9. I. Suemune, L. A. Coldren, M. Yamanishi, and Y. Kan. Appl. Phys. Lett. **53**, 1378 (1978)
10. P. W. A. McIlroy, A. Kurobe, Y. Uematsu. IEEE J. Quantum Electron. **QE-21**, 1666 (1985)
11. A. Kurobe, H. Furuyama, S. Naritsuka, N. Sugiyama, Y. Kokubun, M. Nakamura. IEEE J. Quantum Electron. **QE-24**, 635 (1988)
12. A. Yariv. Appl. Phys. Lett. **53**, 1033 (1988)
13. G. A. Vawter, D. R. Myers, T. M. Brennan, B. E. Hammons. J. P. Hohimer. Electron. Lett. **25 (3)** (1989)
14. D. P. Bour, D. B. Gilbert, L. Elbaum, M. G. Harvey. Appl. Phys. Lett. **53**, 2371 (1988)

15. W. J. Schaff, L. F. Eastman. European MRS Proceedings, **Vol. XVI**, 295 (1987)

16. D. C. Radulescu, W. J. Schaff, L. F. Eastman, J. M. Ballingall, G. O. Ramseyer, S. D. Hersee. J. Vac. Sci. Tech. **B7**, 111 (1989)

17. D. C. Radulescu, G. W. Wicks, W. J. Schaff, A. R. Calawa, and L. F. Eastman. J. Appl. Phys. **62**, 954 (1987)

18. W. J. Schaff, L. F. Eastman, B. van Rees, B. Liles. J. Vac. Sci. Tech. **B2**, 265 (1984)